

Single vibronic level fluorescence spectra from Hagedorn wavepacket dynamics

Zhan Tong Zhang and Jiří J. L. Vaníček^{a)}

Laboratory of Theoretical Physical Chemistry, Institut des Sciences et Ingénierie Chimiques, Ecole Polytechnique Fédérale de Lausanne (EPFL), CH-1015 Lausanne, Switzerland

(Dated: 4 March 2024)

In single vibronic level (SVL) fluorescence experiments, the electronically excited initial state is also excited in one or several vibrational modes. Whereas the time-independent approach of computing all contributing Franck-Condon factors becomes impractical in large systems, a time-dependent formalism has not been applied to simulate emission from arbitrary initial vibrational levels. Here, we apply Hagedorn functions, which are products of a Gaussian and carefully generated polynomials, to represent SVL initial states. Under an at most quadratic potential, the Hagedorn functions are exact solutions to the time-dependent Schrödinger equation and can be propagated using the same equations of motion as a simple Gaussian wavepacket. Having developed an efficient recursive algorithm to compute the overlaps between two Hagedorn wavepackets, we can now evaluate emission spectra from arbitrary vibronic levels using a single trajectory. Here, we use two-dimensional global harmonic models to validate the method by comparing it with quantum split-operator calculations and to demonstrate the effects of displacement, distortion (squeezing), and Duschinsky rotation on SVL spectra. Additionally, we show the practicality of the Hagedorn approach in a high-dimensional system on a displaced, distorted, and Duschinsky-rotated harmonic model with 100 degrees of freedom.

^{a)}Electronic mail: jiri.vanicek@epfl.ch

I. INTRODUCTION

Tuned narrow-band lasers can be used to induce specific vibronic transitions and to prepare a population of molecules excited to a single vibronic level (SVL). The subsequent fluorescence decay of such a system can then be measured and provide important information about excited-state relaxation, higher vibrational structures of the ground state, as well as the vibronic coupling between ground and excited states.^{1–5}

The simulation of SVL spectra of small molecules has been carried out using time-independent sum-over-state expressions,^{6–12} but the computation of Franck-Condon factors in larger molecules becomes challenging with the increasing number of vibrational states involved, especially due to non-separable overlap integrals under Duschinsky mixing effects. A time-dependent approach is more efficient for larger systems and constitutes a more fundamental method that can readily incorporate Duschinsky rotation, Herzberg-Teller,^{13–15} and temperature effects.^{16,17} While time-dependent approaches have been applied to SVL^{18,19} and similar experiments,^{20–22} their practical application has so far been confined to initial states that are singly excited and only in one vibrational mode.

For absorption or emission from the ground vibrational state, the thawed Gaussian approximation^{23–25} (TGA) has been successfully applied to simulate vibrationally resolved electronic spectra in situations where a single Gaussian wavefunction is sufficient to adequately describe the dynamics.^{16,17,26–30} However, the SVL emission process involving a vibrationally excited initial state cannot be described by a single Gaussian wavepacket even at the initial time. Within the harmonic approximation, it may instead be described by a Gaussian multiplied by a polynomial at all times. Tapavicza's generating function approach¹⁹ can treat initial states singly excited in one mode, whereas the extended TGA^{14,31–33} (ETGA) may accommodate simultaneous single excitations in multiple modes, but only in systems without Duschinsky rotation.ⁱ A more general and robust method is needed to address situations where the simultaneous excitation of *multiple* vibrational modes to *higher* levels is involved.

By generalizing Dirac's ladder operators for one-dimensional quantum harmonic oscillators, Hagedorn introduced a special pair of raising and lowering ladder operators in arbitrary

ⁱ With simultaneous multi-mode excitation, although each polynomial factor is linear in its respective dimension, their tensor product is no longer linear. However, without Duschinsky rotation effects, a system remains fully separable at all times and can be treated as several one-dimensional problems.

dimensions that generate a series of functions in the form of a Gaussian wavepacket multiplied by a polynomial.^{34–39} Unlike simple direct products of one-dimensional Hermite functions, Hagedorn functions are exact solutions to the time-dependent Schrödinger equation (TDSE) with a general many-dimensional harmonic potential when the parameters of the associated Gaussian are propagated with classical-like equations of motion. The Hagedorn functions also form a complete orthonormal basis that may be used to expand numerically exact arbitrary solutions to the TDSE with a general potential.⁴⁰ However, in this work, we consider exclusively Hagedorn wavepackets consisting of only one such Hagedorn function at all times. Henceforth, we will use “Hagedorn wavepackets” and “Hagedorn functions” as synonyms.

Despite their promising properties^{38,39,41–43} and a few applications in quantum and chemical physics,^{40,44–48} Hagedorn wavepackets have yet to be applied to spectroscopic simulation, since one important ingredient, an efficient way to compute the correlation functions between two Hagedorn wavepackets, was missing. Having developed an efficient algebraic algorithm for this overlap in Ref. 49, we can now apply the Hagedorn approach to the simulation of SVL spectra.

Here, we first investigate SVL emissions from different vibrational levels in three two-dimensional, two-state harmonic models, examining the effects on spectra due to nuclear displacement, mode distortion (squeezing), and Duschinsky rotation. To validate our approach, we compare the Hagedorn-wavepacket results to “exact” quantum split-operator calculations and, where applicable, the results from (extended) TGA simulations. Importantly, the propagation of Hagedorn wavepackets does not incur any additional computational cost in harmonic potentials beyond that of propagating a single Gaussian wavepacket. The Hagedorn approach is thus suitable for much higher dimensions than grid-based quantum methods. As a demonstration, we compute spectra in a two-state harmonic model system with 100 vibrational degrees of freedom.

II. THEORY

Let $|K\rangle \equiv |e, K\rangle$ denote a specific vibrational state on the potential energy surface of the excited electronic state e , where $K = (K_1, \dots, K_D)$ is the multi-index of non-negative integers specifying the vibrational quantum numbers in the D normal modes. Within the

Condon approximation, the emission rate from $|K\rangle$ to the ground electronic state g may be obtained by the Fourier transform^{13,19,50}

$$\sigma_{\text{em}}(\omega) = \frac{4\omega^3}{3\pi\hbar c^3} |\mu_{ge}|^2 \operatorname{Re} \int_0^\infty \overline{C(t)} \exp[i t(\omega - E_{e,K}/\hbar)] dt \quad (1)$$

of the wavepacket autocorrelation function

$$C(t) = \langle K | \exp(-i\hat{H}_g t/\hbar) | K \rangle. \quad (2)$$

Here, μ_{ge} is the electronic transition dipole moment, \hat{H}_g the nuclear Hamiltonian associated with the ground electronic state, and $E_{e,K} = \hbar\omega_{e,K}$ the vibrational energy of the initial state. In this time-dependent framework, the initial wavepacket is evolved on the ground-state potential energy surface, and the overlaps between the initial wavepacket $|K\rangle$ and the propagated wavepacket $e^{-i\hat{H}_g t/\hbar} |K\rangle$ are computed in order to evaluate the spectrum.

Solving the time-dependent Schrödinger equation is a challenging numerical problem. Hagedorn's semiclassical wavepackets offer a practical approach to evolve a wavepacket in higher-dimensional systems.^{34,37,39} In Hagedorn's parametrization,^{40,51} a normalized D -dimensional Gaussian wavepacket is written as

$$\begin{aligned} \varphi_0[q_t, p_t, Q_t, P_t, S_t](q) &= \frac{1}{(\pi\hbar)^{D/4} \sqrt{\det(Q_t)}} \\ &\quad \times \exp\left(\frac{i}{\hbar} \left(\frac{1}{2} x^T \cdot P_t \cdot Q_t^{-1} \cdot x + p_t^T \cdot x + S_t \right) \right], \end{aligned} \quad (3)$$

with the shifted position $x := q - q_t$, where S_t is a phase factor related to the classical action, q_t and p_t represent the position and momentum of the wavepacket's center, and Q_t and P_t are complex-valued D -dimensional matrices related to the position and momentum covariances. The two matrices replace the “width matrix” $A_t = P_t \cdot Q_t^{-1}$ used in Heller's parametrization^{39,50,51} and satisfy the symplecticity conditions^{38,39}

$$Q_t^T \cdot P_t - P_t^T \cdot Q_t = 0, \quad (4)$$

$$Q_t^\dagger \cdot P_t - P_t^\dagger \cdot Q_t = 2i\text{Id}_D. \quad (5)$$

Hagedorn defined a special pair of raising and lowering operators,

$$A^\dagger \equiv A^\dagger[q_t, p_t, Q_t, P_t] := \frac{i}{\sqrt{2\hbar}} (P_t^\dagger \cdot \hat{x} - Q_t^\dagger \cdot \hat{y}), \quad (6)$$

$$A \equiv A[q_t, p_t, Q_t, P_t] := -\frac{i}{\sqrt{2\hbar}} (P_t^T \cdot \hat{x} - Q_t^T \cdot \hat{y}), \quad (7)$$

where $\hat{x} := \hat{q} - q_t$ and $\hat{y} := \hat{p} - p_t$ are the shifted position and momentum operators. The ladder operators connect the thawed Gaussian wavepacket φ_0 to a family of functions in the form of a Gaussian multiplied by a polynomial, such that

$$\varphi_{K+\langle j \rangle} = \frac{1}{\sqrt{K_j + 1}} A_j^\dagger \varphi_K, \quad (8)$$

$$\varphi_{K-\langle j \rangle} = \frac{1}{\sqrt{K_j}} A_j \varphi_K, \quad (9)$$

where $\langle j \rangle = (0, \dots, 1, \dots, 0)$ is the j -th unit vector in D dimensions.^{34,37-39} In general, the polynomial factor cannot be expressed as a tensor product of univariate polynomials.^{36,39,53,54}

However, in the special case where $Q_t^{-1} \cdot \overline{Q_t}$ is diagonal, it can be represented as a tensor product of scaled Hermite polynomials.³⁹ If we adopt the mass-weighted normal-mode coordinates on the excited-state potential energy surface, the “position” matrix Q_0 of the initial state may be chosen to be diagonal with $Q_{0,jj} = \omega_j^{-1/2}$, where ω_j is the angular frequency of the j -th vibrational mode. In this case, the initial Hagedorn function

$$\varphi_K(q) = \langle q | K \rangle = \frac{\varphi_0(q)}{\sqrt{2^{|K|} K!}} \prod_{j=1}^D H_{K_j} \left(\sqrt{\frac{\omega_j}{\hbar}} \cdot x_j \right) \quad (10)$$

is exactly the vibrational eigenfunction of a harmonic Hamiltonian and can thus represent the SVL initial state.

Notably, in a harmonic potential

$$V(q) = v_0 + (q - q_{\text{ref}})^T \cdot \kappa \cdot (q - q_{\text{ref}})/2, \quad (11)$$

Hagedorn wavepackets, like thawed Gaussians, are exact solutions to the time-dependent Schrödinger equation. The parameters of the Gaussian associated with the Hagedorn wavepacket evolve according to the equations

$$\dot{q}_t = m^{-1} \cdot p_t, \quad (12)$$

$$\dot{p}_t = -V'(q_t) \quad (13)$$

$$\dot{Q}_t = m^{-1} \cdot P_t, \quad (14)$$

$$\dot{P}_t = -V''(q_t) \cdot Q_t, \quad (15)$$

$$\dot{S}_t = L_t, \quad (16)$$

which are the same as the equations for propagating a Gaussian wavepacket.^{37,39,51} Here, the subscript t denotes the time, m the real symmetric mass matrix (scalar in mass-weighted

normal-mode coordinates), and L_t is the Lagrangian. Remarkably, with Hagedorn wavepackets, the SVL emission from *any* vibrational level can be evaluated from the same trajectory $(q_t, p_t, Q_t, P_t, S_t)$ at zero cost beyond propagating a simple Gaussian.

To finally obtain SVL spectra from the dynamics results, the evaluation of overlap integrals (2) between two Hagedorn wavepackets with different Gaussian parameters is needed. However, a straightforward analytical expression, like that available for overlaps between two Gaussian wavepackets, has remained elusive for Hagedorn wavepackets. Past applications of Hagedorn wavepackets require numerical quadrature for integrals, which becomes challenging in higher dimensions.^{40,44–48} In Ref. 49, we have proposed instead a recursive algebraic scheme to compute these overlaps. This allows us to apply Hagedorn wavepackets in much higher dimensions, paving the way for their spectroscopic applications. The cost of computing the overlaps becomes negligible compared to the costly polyatomic electronic structure calculations, which only need to be carried out once for the central Gaussian trajectory, and do not have to be repeated for the vibrationally excited initial states.

Hagedorn wavepackets can be seen as a generalization of coherent states,^{37,41,54,55} and our approach is thus connected to the generating function formalism proposed by Huh and Berger.¹⁸ Although their expressions, relying on multivariate Hermite polynomials, are also general for arbitrary initial vibrational levels, no implementation or application was given. As far as we know, the only practical formulation is that of Tapavicza,¹⁹ which is so far limited to single excitation in one mode. The Hagedorn approach, in addition to its generality, also provides a more intuitive time-dependent picture and offers a straightforward propagation scheme.

In this study, we focus solely on harmonic models so that the results can be analyzed without additional approximation or errors. Furthermore, global harmonic potentials have served as a useful starting point for modeling many molecules and have been used with success to simulate vibronic spectra.^{6,19,56,57}

III. NUMERICAL EXAMPLES

A. Two-dimensional harmonic potentials

To demonstrate the Hagedorn approach in the simplest multi-dimensional cases, we start with two-dimensional models so that “exact” quantum calculations are readily accessible for the verification of the results.

We assume that the initial, excited-state electronic surface V_e and the final, ground-state electronic surface V_g can both be described by a quadratic function (11). The ground-state surface V_g is centered around zero, i.e., $q_{\text{ref},g} = (0, 0)$. In all cases, the initial wavepacket is centered at $q_0 = q_{\text{ref},e} = (15, -15)$, i.e. at the minimum of the excited-state surface V_e , and has zero momentum $p_0 = (0, 0)$.

Keeping V_e the same in all cases, we then construct three different ground-state surfaces V_g to demonstrate the effects of mode displacement, distortion, and Duschinsky rotation in a cumulative fashion. In each case, a Gaussian wavepacket corresponding to the ground vibrational state of V_e is propagated for 40000 a.u. (20000 steps with a time step of 2 a.u.) on the surface V_g . For each system, we provide examples of emissions from various vibrational levels, including the ground vibrational level, a singly excited level, a level with higher excitations in one mode, and two levels with multi-mode excitations. Specifically, we simulate SVL spectra from initial vibrational levels $1^a 2^b$, $(a, b) \in \{(0, 0), (1, 0), (0, 3), (1, 1)(2, 1)\}$, where a, b denote the vibrational quantum numbers in modes 1 and 2 of the excited electronic state.

The autocorrelation function of the Hagedorn wavepacket associated with each initial vibrational level is computed every two steps using the overlap expressions derived in Ref. 49. The SVL emission spectra are then evaluated by Fourier transforming the autocorrelation functions multiplied with a Gaussian damping function, which results in a spectral broadening with a half-width at half-maximum of 50 cm^{-1} .

Figure 1 contains the SVL emission spectra of the three systems computed using Hagedorn wavepackets. The spectral intensities in all spectra are scaled by the highest peak of the $1^0 2^0$ spectrum in the displaced, distorted and rotated system, which can be considered as the most comprehensive harmonic description of a real, anharmonic system. The other two systems can be then thought of as simplified approximations of the full harmonic system.

Each spectrum is shifted so that the transition to the vibrational ground state ($1_0^a 2_0^b$, where the subscripts denote the final vibrational quantum numbers in the ground electronic state after the transition) is at 0 cm^{-1} .

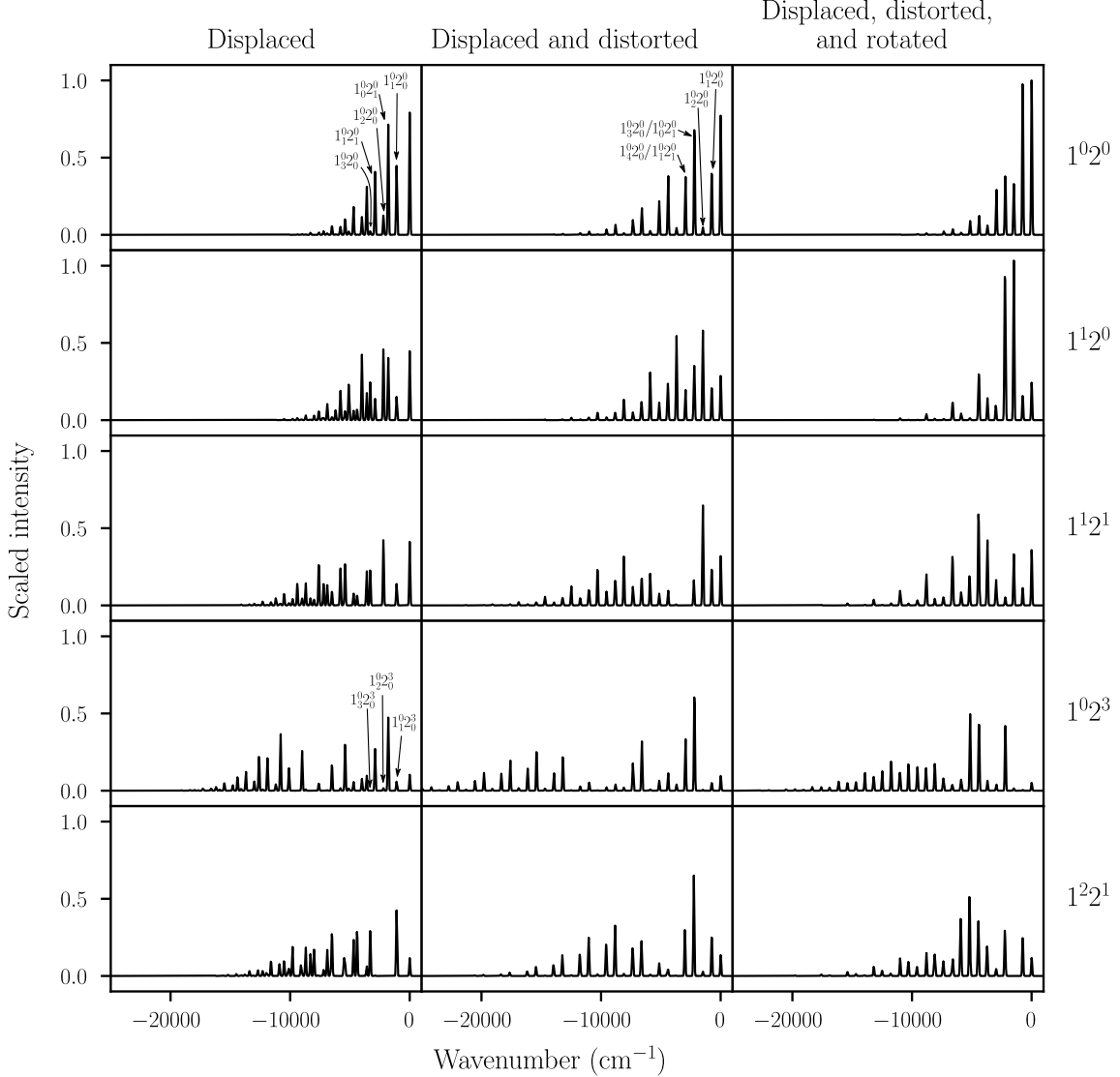


FIG. 1: Simulated SVL emission spectra of three two-dimensional two-level harmonic systems from five different initial vibrational levels (indicated by the labels on the right).

If the ground- and excited-state surfaces were identical (up to a constant energy gap v_0), the resulting spectrum would consist of a single peak at a wavenumber corresponding to the electronic energy gap. Only transitions with $\Delta v = 0$ ($1_a^a 2_b^b$) would be allowed since

the vibrational wavefunctions with different vibrational quantum numbers v in the two electronic states would be orthogonal to each other. The horizontal displacement between the two electronic surfaces breaks this symmetry and allows for more vibronic transitions.

In the displacement-only system (first column in Fig. 1), the two displaced surfaces V_g and V_e have the same diagonal Hessian matrix $\kappa_g = \kappa_e$ corresponding to vibrational wavenumbers $\tilde{\nu}_1'' = 1100 \text{ cm}^{-1}$ and $\tilde{\nu}_2'' = 1800 \text{ cm}^{-1}$. Without Duschinsky rotation, the vibronic spectrum is the convolution of the spectrum in each vibrational degree of freedom. Consequently, the spectral peaks for transitions $1_\alpha^a 2_\beta^b$ appear at $\alpha\tilde{\nu}_1'' + \beta\tilde{\nu}_2''$, where $\alpha, \beta \in \mathbb{N}_0$.

The intensity pattern of the SVL spectra is significantly influenced by the initial wavepacket. Higher vibrational excitations in the initial state generally result in more transitions to higher vibrational states on the ground electronic surface, whereas the specific initial excitation allows the selective enhancement (or attenuation) of peaks. For example, in the 1^02^3 spectrum, significant peaks appear in the $< -8000 \text{ cm}^{-1}$ region, whereas the v_1'' ($\beta = 0$) peaks, e.g., $1_1^0 2_0^3$, $1_2^0 2_0^3$, and $1_3^0 2_0^3$ (labeled on spectra), are considerably attenuated compared to the 1^02^0 spectrum (e.g., peaks $1_1^0 2_0^0$, $1_2^0 2_0^0$, and $1_3^0 2_0^0$). The sensitivity of SVL spectra to the initial excitation provides a valuable tool for understanding the vibronic structure in complex molecular systems.

If the ground and excited electronic surfaces no longer have the same corresponding vibrational frequencies, the so-called “mode distortion” leads to changes in peak positions as well as in intensity (second column in Fig. 1) in addition to the effects from displacement. In the displaced and distorted system, the initial wavepackets are kept the same, but V_g now has a diagonal Hessian matrix $\kappa_{g,\text{distorted}}$ corresponding to vibrational wavenumbers $\tilde{\nu}_1'' = 750 \text{ cm}^{-1}$ and $\tilde{\nu}_2'' = 2200 \text{ cm}^{-1}$. As the ground electronic surface changes, the possible peak positions adapt accordingly at the combination of new frequencies, which can be observed by comparing the ordering and positions of the labeled peaks on the 1^02^0 spectra in the first and second columns. In this particular case, since $\tilde{\nu}_2'' \approx 3\tilde{\nu}_1''$, the spectral peaks exhibit a more regular spacing, and certain broadened peaks, e.g. for $1_3^0 2_0^0$ and $1_0^0 2_1^0$ (labeled together on the 1^02^0 spectrum), actually overlap in this displaced and distorted system. The mode distortion also alters the intensity pattern, which is particularly evident in the 1^12^1 and 1^22^1 spectra (compare the first and second columns).

Finally, in the Duschinsky-rotated system (third column in Fig. 1), V_g is modified so that

$\kappa_{g,\text{rotated}} = R(20^\circ) \cdot \kappa_{g,\text{distorted}}$, where

$$R(\theta) = \begin{pmatrix} \cos \theta, & -\sin \theta \\ \sin \theta, & \cos \theta \end{pmatrix} \quad (17)$$

is a rotation matrix. The analysis of spectra here becomes more challenging, even in two-dimensional systems. We observe significant differences in the intensity pattern compared to unrotated systems. In our particular case, the frequency range of the spectral region also appears to be decreased. From a time-independent perspective, this could be explained by the fact that the Duschinsky rotation reduces the overlaps or Franck-Condon factors between the initial wavepacket and higher vibrational states on the ground electronic surface. It is worth noting that in this most general harmonic model, the Hagedorn wavepackets do not maintain the separable form of (10) during propagation, since Q_t is no longer diagonal when evolved under a Duschinsky-rotated potential. With Hagedorn's ingenious construction, the propagation algorithm maintains its simplicity even for general, non-separable Hagedorn wavepackets, which are not simply tensor products of eigenfunctions of one-dimensional harmonic oscillators.

In order to validate the Hagedorn approach, we also propagated the initial states using the second-order Fourier split-operator algorithm with 256×256 grid points; however, unlike the Hagedorn approach, the quantum dynamics must be performed separately for *each* initial vibrational level in each system. Where applicable, the spectra were also evaluated using the TGA^{23,25,50} (for 1^02^0) and its extended version^{14,31} (for 1^12^0 and 1^12^1). We compare the spectra obtained using Hagedorn wavepackets to the results from “exact” quantum calculations as well as (extended) TGA simulations in Fig. 2. Before calculating the differences, the spectra were all scaled and shifted as in Fig. 1. As expected, we observe excellent agreement between the methods. The comparison with the (extended) TGA calculations, which are performed in Heller's parametrization^{23,51} of the Gaussian, which is substantially different from Hagedorn's, serves as a further validation. In addition, ETGA employs a different approach to propagate the linear polynomial factor.

A notable advantage of Hagedorn wavepackets over the ETGA and the previously reported generating function approach¹⁹ is their ability to simulate dynamics starting from arbitrary initial vibrational levels, going beyond linear polynomial factors. Among the examples shown, the ETGA approach can compute emission from the 1^12^1 vibrational level

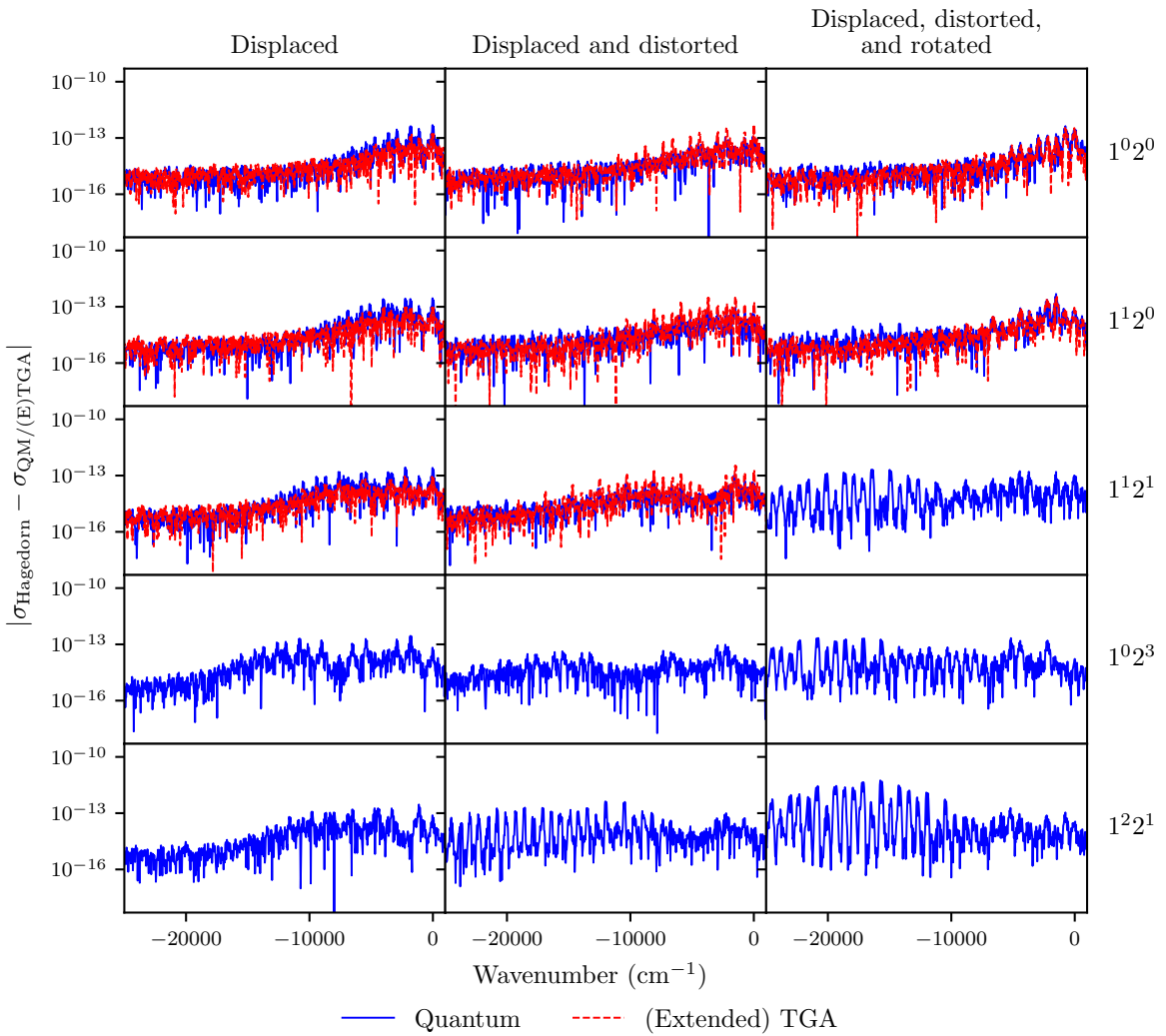


FIG. 2: Absolute differences between scaled spectra computed using Hagedorn wavepackets (Fig. 1) and those obtained with the quantum split-operator algorithm (QM, blue) or (extended) thawed Gaussian approximation [(E)TGA, red].

only for cases without Duschinsky rotation, where the system can be separated into two one-dimensional systems each with at most a single excitation. The 1^12^1 spectra are then computed using the correlation function obtained by multiplying the correlation functions from the two one-dimensional systems.

B. 100-dimensional displaced, distorted, and Duschinsky-rotated harmonic system

In higher dimensions, the quantum split-operator approach quickly becomes unfeasible due to the curse of dimensionality, particularly when treating excited vibrational wavefunctions for which denser grids are generally needed. In contrast, Hagedorn wavepackets circumvent the need for a grid and can be efficiently propagated within a harmonic approximation using the same trajectory as the simple thawed Gaussian. With the algebraic expressions developed in Ref. 49, we can now use Hagedorn wavepackets in much higher dimensions.

Figure 3 shows SVL emission spectra in a 100-dimensional system that incorporates displacement, distortion, and Duschinsky rotation effects. Except for the potential energy surface and initial wavepackets, the computation parameters (time step, total time of propagation, frequency of evaluation of the autocorrelation function, broadening of the spectra) are identical to those for the two-dimensional systems. We choose two modes (namely modes 30 and 40) to be vibrationally excited in the initial wavepackets, computing emission spectra from initial vibrational levels 30^a40^b , with the same set of (a, b) as in the two-dimensional cases.

The spectra become significantly more complex in higher-dimensional systems. We observe broadened tails in the lower frequency region, which are likely attributable to the effects of Duschinsky rotation here (compare to Fig. 4). This also demonstrates the advantage of the time-dependent approach, where Duschinsky rotation can be intrinsically taken into account, in contrast to the time-independent method, which faces challenges related to the pre-selection of likely transitions and the computation of non-separable Franck-Condon integrals in high-dimensional systems.

IV. CONCLUSIONS

We have demonstrated that Hagedorn wavepackets offer a robust approach to simulate SVL emission spectra of polyatomic molecules in the harmonic approximation, naturally accounting for mode distortion and Duschinsky rotation effects. Using a single thawed Gaussian trajectory in each system, we were able to evaluate the emission spectra from any

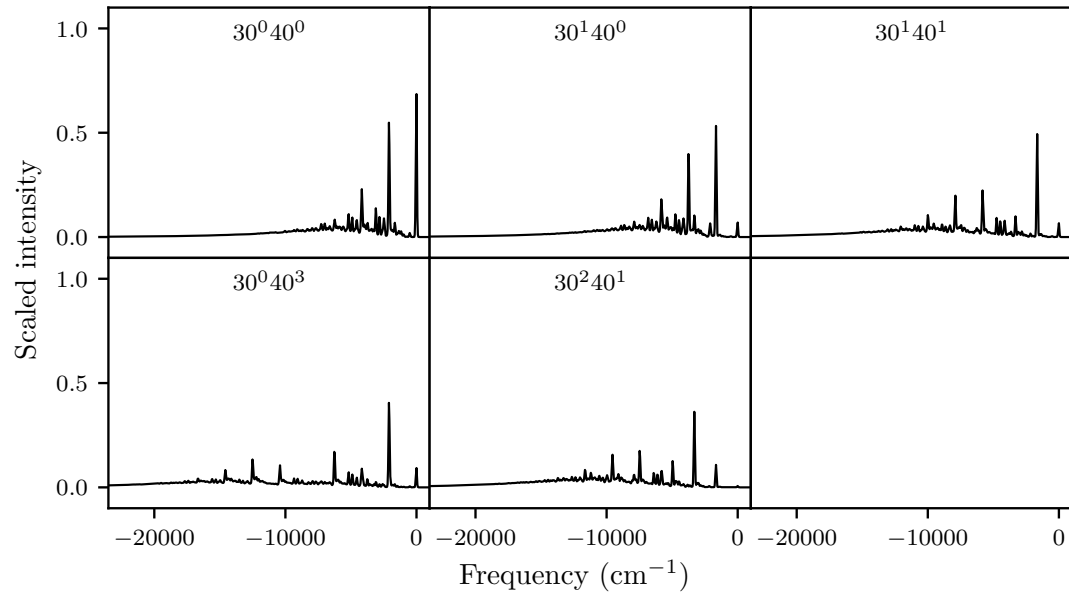


FIG. 3: SVL emission spectra from different vibrational levels (indicated in each panel) in a 100-dimensional two-state displaced, distorted, and Duschinsky-rotated harmonic system.

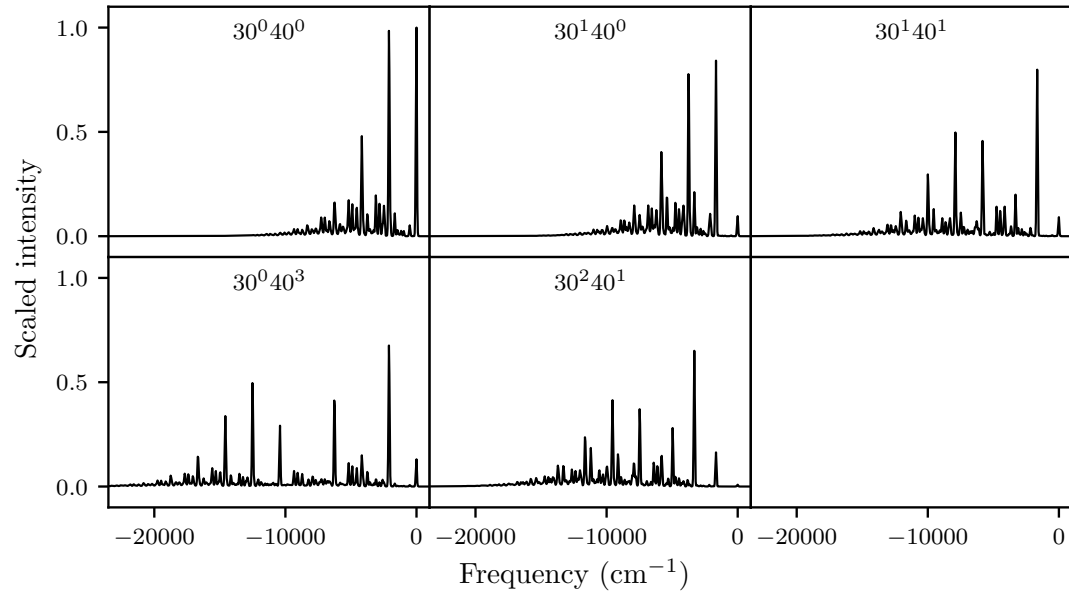


FIG. 4: SVL emission spectra from different vibrational levels (indicated in each panel) in a 100-dimensional two-state displaced and distorted harmonic system (without Duschinsky rotation).

vibrational level without incurring additional propagation cost over that required for simulating emission from the ground level. Evaluating the overlaps, the cost of which becomes negligible in *ab initio* applications, represents the only additional step. The excellent agreement between the Hagedorn and grid-based quantum results in two-dimensional examples validates the algebraic expressions we had developed for the overlaps between two general Hagedorn wavepackets.⁴⁹ On a 100-dimensional example, we have also demonstrated the feasibility of using Hagedorn wavepackets and our overlap expressions in high-dimensional systems.

In conclusion, Hagedorn wavepackets are well suited for simulating SVL emission spectra. While the present work only considered model potentials, Hagedorn wavepackets can readily be applied to realistic molecular systems using harmonic potentials constructed from *ab initio* electronic structure calculations. Moreover, as in the thawed Gaussian approximation for computing ground-state emission spectra, anharmonicity effects could be partially captured by propagating Hagedorn wavepackets within local harmonic approximation using on-the-fly *ab initio* data.

Furthermore, the Hagedorn approach presented here could also be adapted to other spectroscopy techniques where the initial state is vibrationally excited or otherwise cannot be adequately described by a single Gaussian wavepacket, such as in the case of vibrationally promoted electronic resonance (VIPER) experiments^{21,22,58} or fluorescence-encoded infrared (FEIR) spectroscopy.⁵⁹

V. ACKNOWLEDGEMENTS

The authors acknowledge the financial support from the European Research Council (ERC) under the European Union’s Horizon 2020 Research and Innovation Programme (Grant Agreement No. 683069–MOLEQULE) and from the EPFL.

REFERENCES

- ¹S. M. Beck, J. B. Hopkins, D. E. Powers, and R. E. Smalley, *J. Chem. Phys.* **74**, 43 (1981).
- ²T. A. Stephenson, P. L. Radloff, and S. A. Rice, *J. Chem. Phys.* **81**, 1060 (1984).

³W. R. Lambert, P. M. Felker, J. A. Syage, and A. H. Zewail, *J. Chem. Phys.* **81**, 2195 (1984).

⁴T. M. Woudenberg, S. K. Kulkarni, and J. E. Kenny, *J. Chem. Phys.* **89**, 2789 (1988).

⁵J. A. Nicholson, W. D. Lawrence, and G. Fischer, *Chemical Physics* **196**, 327 (1995).

⁶F.-T. Chau, J. M. Dyke, E. P.-F. Lee, and D.-C. Wang, *J. Electron Spectrosc. Relat. Phenom.* **97**, 33 (1998).

⁷F.-T. Chau, J. M. Dyke, E. P. F. Lee, and D. K. W. Mok, *J. Chem. Phys.* **115**, 5816 (2001).

⁸R. Grimminger, D. J. Clouthier, R. Tarroni, Z. Wang, and T. J. Sears, *J. Chem. Phys.* **139**, 174306 (2013).

⁹D. K. W. Mok, E. P. F. Lee, F.-T. Chau, and J. M. Dyke, *J. Chem. Phys.* **140**, 194311 (2014).

¹⁰D. K. W. Mok, E. P. F. Lee, and J. M. Dyke, *J. Chem. Phys.* **144**, 184303 (2016).

¹¹R. Tarroni and D. J. Clouthier, *J. Chem. Phys.* **153**, 014301 (2020).

¹²T. C. Smith, M. Gharaibeh, and D. J. Clouthier, *J. Chem. Phys.* **157**, 204306 (2022).

¹³A. Baiardi, J. Bloino, and V. Barone, *J. Chem. Theory Comput.* **9**, 4097 (2013).

¹⁴A. Patoz, T. Begušić, and J. Vaníček, *J. Phys. Chem. Lett.* **9**, 2367 (2018).

¹⁵A. Prlj, T. Begušić, Z. T. Zhang, G. C. Fish, M. Wehrle, T. Zimmermann, S. Choi, J. Roulet, J.-E. Moser, and J. Vaníček, *J. Chem. Theory Comput.* **16**, 2617 (2020).

¹⁶T. Begušić and J. Vaníček, *J. Chem. Phys.* **153**, 024105 (2020).

¹⁷T. Begušić and J. Vaníček, *J. Phys. Chem. Lett.* **12**, 2997 (2021).

¹⁸J. Huh and R. Berger, *Journal of Physics: Conference Series* **380**, 012019 (2012).

¹⁹E. Tapavicza, *J. Phys. Chem. Lett.* **10**, 6003 (2019).

²⁰A. Baiardi, J. Bloino, and V. Barone, *J. Chem. Phys.* **141** (2014), 10.1063/1.4895534.

²¹J. Von Cosel, J. Cerezo, D. Kern-Michler, C. Neumann, L. J. G. W. Van Wilderen, J. Bredenbeck, F. Santoro, and I. Burghardt, *J. Chem. Phys.* **147**, 164116 (2017).

²²M. Horz, H. M. A. Masood, H. Brunst, J. Cerezo, D. Picconi, H. Vormann, M. S. Niranhatam, L. J. G. W. Van Wilderen, J. Bredenbeck, F. Santoro, and I. Burghardt, *J. Chem. Phys.* **158**, 064201 (2023).

²³E. J. Heller, *J. Chem. Phys.* **62**, 1544 (1975).

²⁴F. Grossmann, *J. Chem. Phys.* **125**, 014111 (2006).

²⁵M. Wehrle, M. Šulc, and J. Vaníček, *J. Chem. Phys.* **140**, 244114 (2014).

²⁶M. Wehrle, S. Oberli, and J. Vaníček, *J. Phys. Chem. A* **119**, 5685 (2015).

²⁷T. Begušić, J. Roulet, and J. Vaníček, *J. Chem. Phys.* **149**, 244115 (2018).

²⁸T. Begušić, M. Cordova, and J. Vaníček, *J. Chem. Phys.* **150**, 154117 (2019).

²⁹T. Begušić and J. Vaníček, *J. Chem. Phys.* **153**, 184110 (2020).

³⁰T. Begušić, E. Tapavicza, and J. Vaníček, *J. Chem. Theory Comput.* **18**, 3065 (2022).

³¹S.-Y. Lee and E. J. Heller, *J. Chem. Phys.* **76**, 3035 (1982).

³²T. Begušić, A. Patoz, M. Šulc, and J. Vaníček, *Chem. Phys.* **515**, 152 (2018).

³³M. Wenzel and R. Mitric, *J. Chem. Phys.* **158**, 034105 (2023).

³⁴G. A. Hagedorn, *Commun. Math. Phys.* **71**, 77 (1980).

³⁵G. A. Hagedorn, *Ann. Phys. (NY)* **135**, 58 (1981).

³⁶G. A. Hagedorn, *Ann. Henri Poincaré* **42**, 363 (1985).

³⁷G. A. Hagedorn, *Ann. Phys. (NY)* **269**, 77 (1998).

³⁸C. Lubich, *From Quantum to Classical Molecular Dynamics: Reduced Models and Numerical Analysis*, 12th ed. (European Mathematical Society, Zürich, 2008).

³⁹C. Lasser and C. Lubich, *Acta Numerica* **29**, 229 (2020).

⁴⁰E. Faou, V. Gradinaru, and C. Lubich, *SIAM J. Sci. Comp.* **31**, 3027 (2009).

⁴¹C. Lasser and S. Troppmann, *J. Fourier Anal. Appl.* **20**, 679 (2014).

⁴²H. Dietert, J. Keller, and S. Troppmann, *J. Math. Anal. Appl.* **450**, 1317 (2017).

⁴³T. Ohsawa, *Nonlinearity* **31**, 1807 (2018).

⁴⁴V. Gradinaru, G. A. Hagedorn, and A. Joye, *J. Chem. Phys.* **132**, 184108 (2010).

⁴⁵R. Bourquin, V. Gradinaru, and G. A. Hagedorn, *J. Math. Chem.* **50**, 602 (2012).

⁴⁶E. Kieri, S. Holmgren, and H. O. Karlsson, *J. Chem. Phys.* **137**, 044111 (2012).

⁴⁷Z. Zhou, *J. Comput. Phys.* **272**, 386 (2014).

⁴⁸V. Gradinaru and O. Rietmann, *J. Comput. Phys.* **445**, 110581 (2021).

⁴⁹Z. T. Zhang and J. Vaníček, “Algebraic evaluation of overlap integrals between hagedorn basis functions in higher dimensions,” (2024), in preparation.

⁵⁰E. J. Heller, *Acc. Chem. Res.* **14**, 368 (1981).

⁵¹J. J. L. Vaníček, *J. Chem. Phys.* **159**, 014114 (2023).

⁵²E. J. Heller, *J. Chem. Phys.* **75**, 2923 (1981).

⁵³G. A. Hagedorn, *Ann. Phys. (NY)* **362**, 603 (2015).

⁵⁴T. Ohsawa, *J. Fourier Anal. Appl.* **25**, 1513 (2019).

⁵⁵M. Combescure, *J. Math. Phys.* **33**, 3870 (1992).

⁵⁶F. Santoro, R. Improta, A. Lami, J. Bloino, and V. Barone, *J. Chem. Phys.* **126**, 084509 (2007).

⁵⁷F. Santoro, A. Lami, R. Improta, J. Bloino, and V. Barone, *J. Chem. Phys.* **128**, 224311 (2008).

⁵⁸L. J. G. W. van Wilderen, A. T. Messmer, and J. Bredenbeck, *Angew. Chem. Int. Ed.* **53**, 2667 (2014).

⁵⁹L. Whaley-Mayda, A. Guha, S. B. Penwell, and A. Tokmakoff, *J. Am. Chem. Soc.* **143**, 3060 (2021).